https://ntrs.nasa.gov/search.jsp?R=19930009686 2020-03-17T07:22:37+00:00Z

3-1-93
E-6663

NASA Technical Memorandum 105272

Structural Dynamic Testing of Composite Propfan Blades for a Cruise Missile Wind Tunnel Model

Stephen D. Elgin and Thomas J. Sutliff
Lewis Research Center
Cleveland, Ohio

February 1993

NASA

STRUCTURAL DYNAMIC TESTING OF COMPOSITE PROPFAN BLADES FOR A CRUISE MISSILE WIND TUNNEL MODEL

Stephen D. Elgin and Thomas J. Sutliff
National Aeronautics and Space Administration
Lewis Research Center
Cleveland, Ohio 44135

Summary

The Naval Weapons Center at China Lake, California is currently evaluating a counterrotating propfan system as a means of propulsion for the next generation of cruise missiles. The details and results of a structural dynamic test program are presented for scale model graphite-epoxy composite propfan blades. These blades are intended for use on a cruise missile wind tunnel model. Both the dynamic characteristics and demonstrated strain operating limits of the blades are presented. Complications associated with high strain level fatigue testing methods are also discussed.

Introduction

The Department of the Navy Long Range Conventional Standoff Weapon (LRCSW) Program Office is investigating applied technologies for use in the next generation of cruise missiles. One technology being investigated for the propulsion of future cruise missiles is an unducted fan (ref. 1). An artist's conception of an advanced cruise missile with unducted fan propulsion is shown in figure 1. In support of this technology evaluation, a joint DOD/NASA wind tunnel test program has been initiated. The wind tunnel program will evaluate the installed characteristics of propfans on a 55-percent scale cruise missile model in the NASA Ames 14-ft transonic wind tunnel.

The NASA Lewis Research Center has developed two propfan blade designs, designated CM-1D and CM-2D, for evaluation in the wind tunnel tests. Both designs consist of two counterrotating fans, each with six blades. The designs for the forward and aft counterrotating fans differ.

Dynamic Test Program

The NASA Lewis development program involved the design, analysis, fabrication, and engineering evaluation testing of the blade designs. One aspect of the engineering evaluation was a dynamic test program for which two goals were established. The first goal was to characterize the as-built dynamics of the blades. The dynamic characteristics of interest were the first four blade resonant frequencies and corresponding modal strain ratios. The modes of interest were determined by analysis to be in the range of 300 to 4000 Hz (refs. 2 and 3). The modal strain ratios are response strain measurements normalized with respect to a reference strain level at a resonant condition. The second goal was to demonstrate an acceptable maximum strain operating limit for each blade design that could then be used during the wind tunnel tests. A strain level of 1200 microstrain was chosen as the limit amplitude. The accumulation of 10 million cycles without failure was the chosen criterion to demonstrate operating durability at the limit strain amplitude. The limit strain amplitude and duration were selected based both on experience with composite propfan blade test programs and on the published useful life limits of the strain gauges (refs. 4 and 5). The failure of a blade was defined as a 10 percent decrease in any of the first four resonant frequencies after exposure to the limit strain amplitude and duration.

This failure criterion was selected based on the need to limit changes in the blade stiffness due to accumulated fatigue damage. Such changes could result in aeroelastic instabilities during the wind tunnel testing.

The dynamic testing was conducted in two segments to accomplish these goals. In the first, a single-axis sine-sweep resonance survey was performed on each blade design to establish the as-built dynamic characteristics. In the second segment, a sinusoidal excitation dwell test was

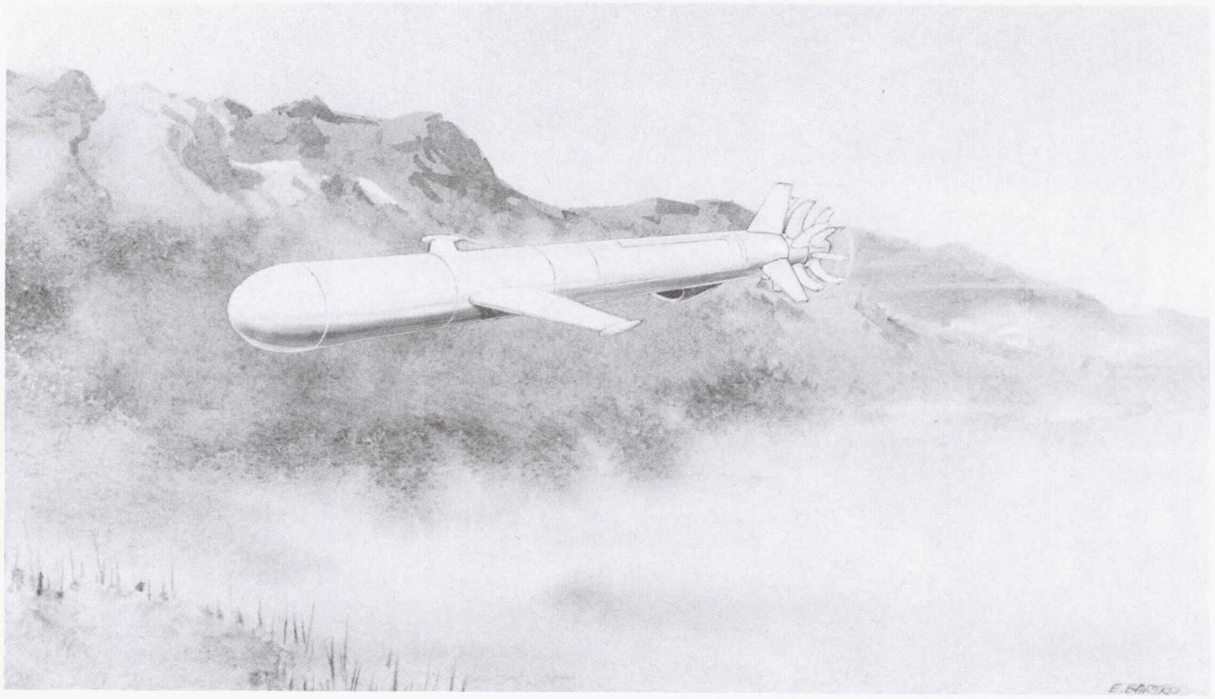

Figure 1.—LRCSW cruise missile concept.

conducted to verify that the chosen operating limits were acceptable.

Test Hardware

The blades for both designs are constructed of laminated composite materials. Each blade was fabricated using plies of T300 graphite fiber in a 250 °F cure epoxy matrix. Typical blade construction is illustrated in figure 2. Note that there is no metallic spar. The blade base stem terminates in a metallic shank shell that is retained in the hub of the propulsion system.

Each blade (CM-1D forward, CM-1D aft, CM-2D forward, and CM-2D aft) was instrumented on its airfoil surface with four general-purpose single-element strain gauges. The strain-gauge locations were chosen based on analytical predictions of principal strain distribution (refs. 2 and 3). Each of the four locations and orientations corresponds to the position and direction of the predicted maximum principal strain for each of the first four modes of each blade. Strain-gauge placement for each blade is shown in figures 3 to 6.

The strain gauges and lead wires were bonded to the blade surfaces with an adhesive. The lead wires were routed along the blade surface, through a small hole drilled in the blade base, and out the bottom of the base.

Blade Fixture

The interface fixture between the blade test specimens and the excitation source (an electrodynamic shaker) was

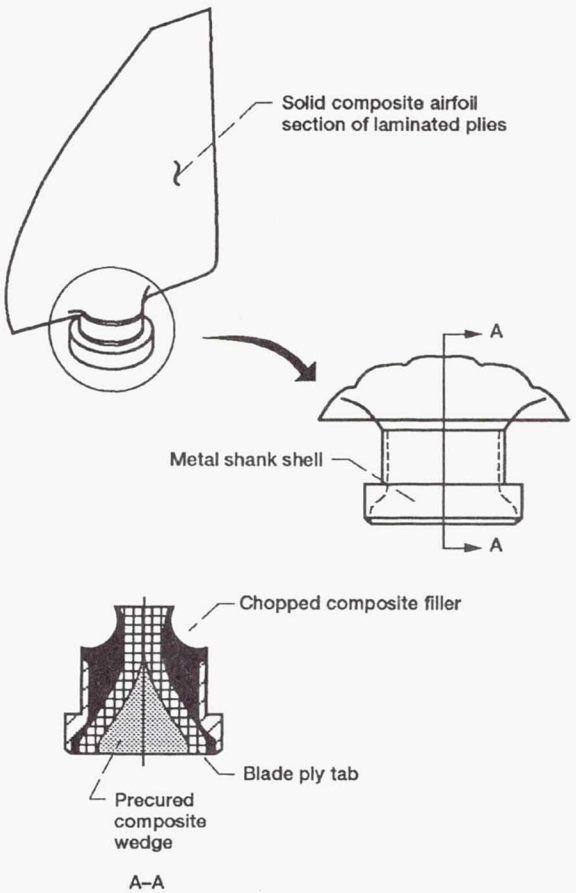

Figure 2.—Typical CM series blade construction.

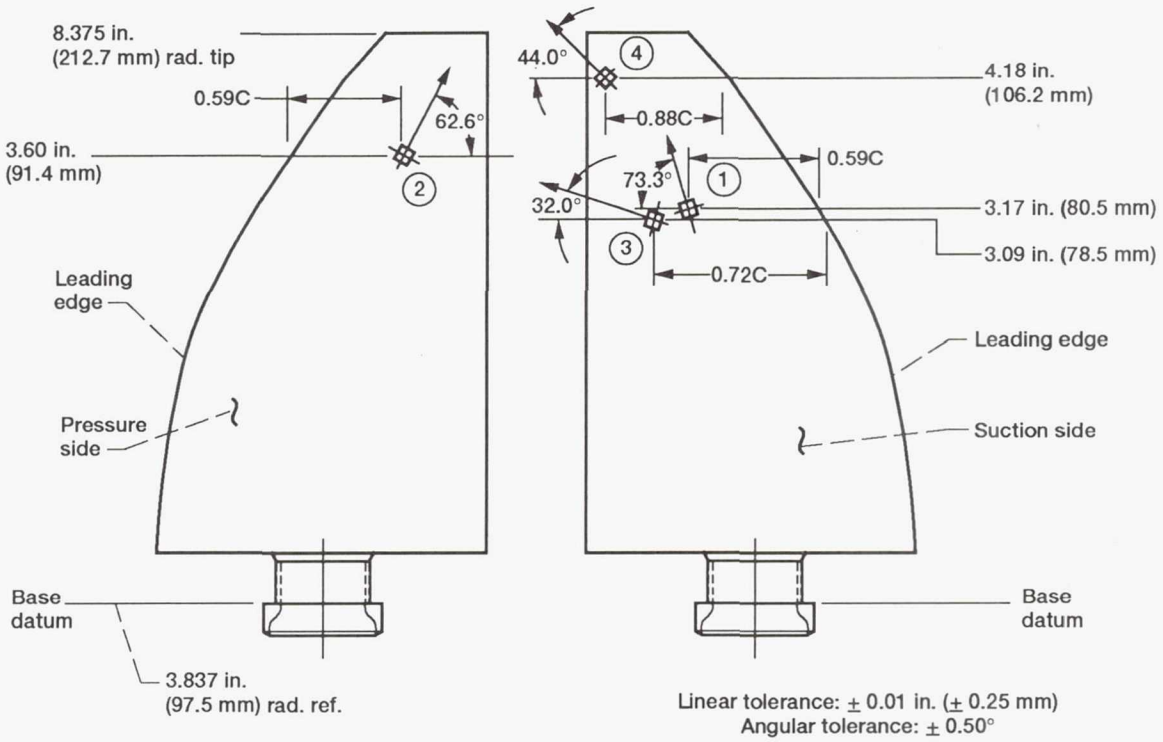

Figure 3.—CM-1D forward blade instrumentation. Arrows indicate orientation of strain gauge. Dimension from leading edge to gauge location is in fraction of chord (C). Dimension from base datum to gauge location is radial (R).

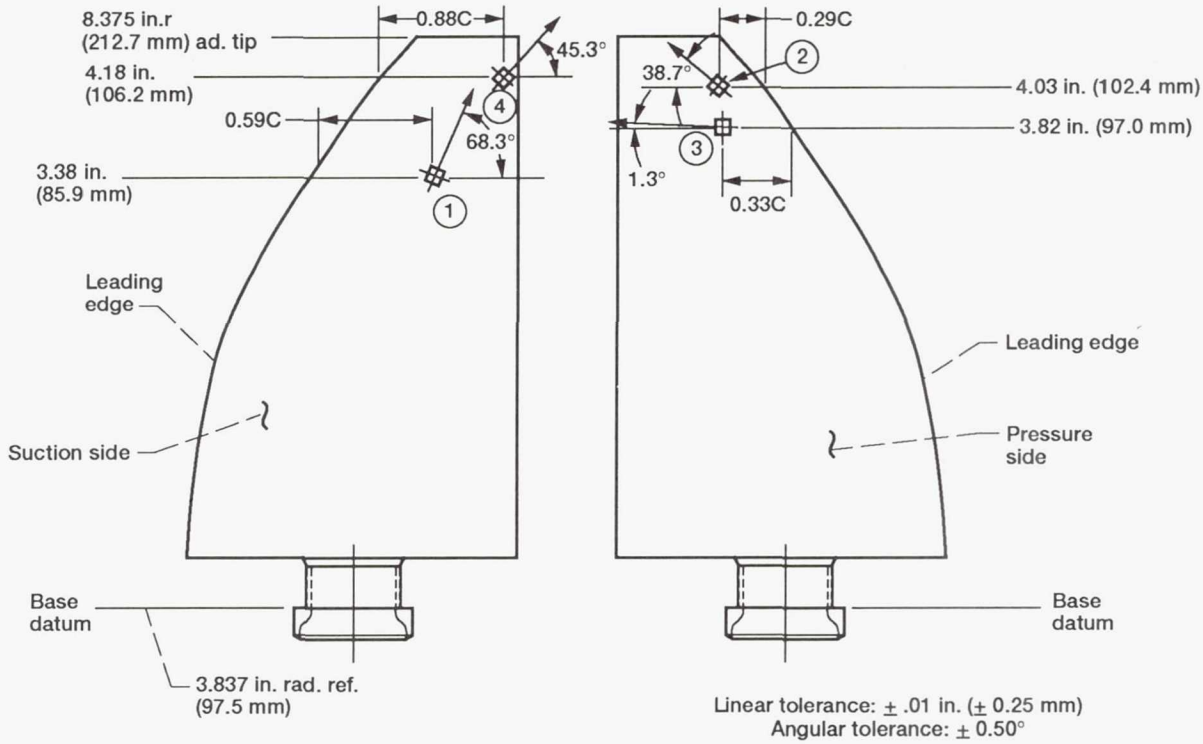

Figure 4.—CM-1D aft blade instrumentation. Arrows indicate orientation of strain gauge. Dimension from leading edge to gauge location is in fraction of chord (C). *Dimension from base datum to gauge location is radial (R).*

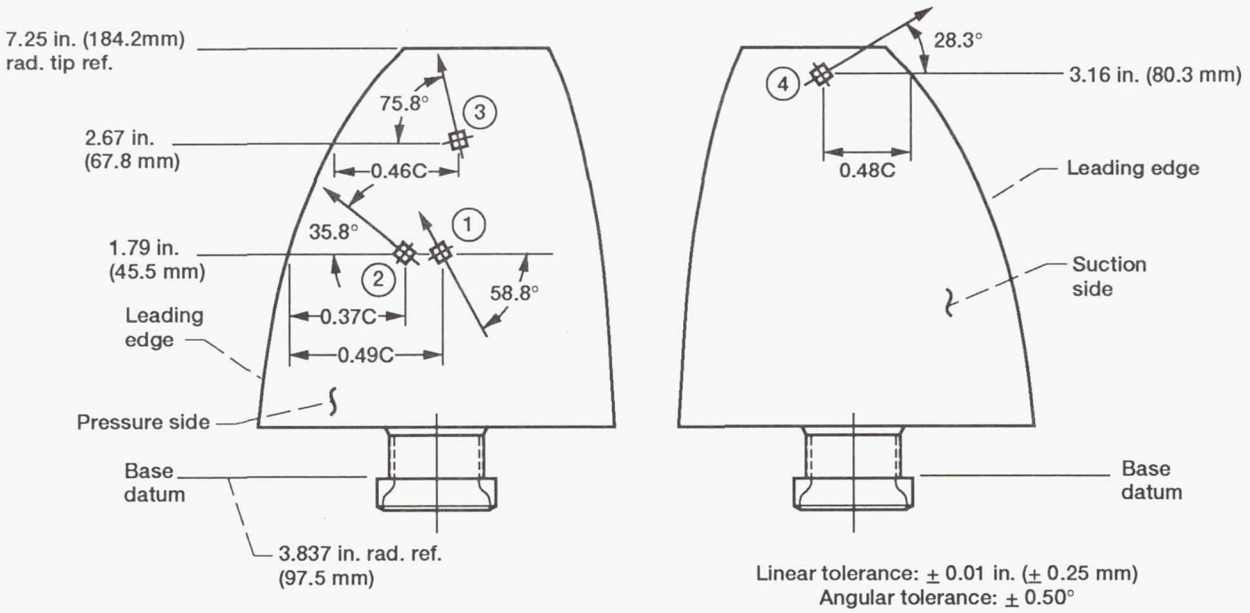

Figure 5.—CM-2D forward blade instrumentation. Arrows indicate orientation of strain gauge. Dimension from leading edge to gauge location is in fraction of chord (C). Dimension from base datum to gauge location is radial (R).

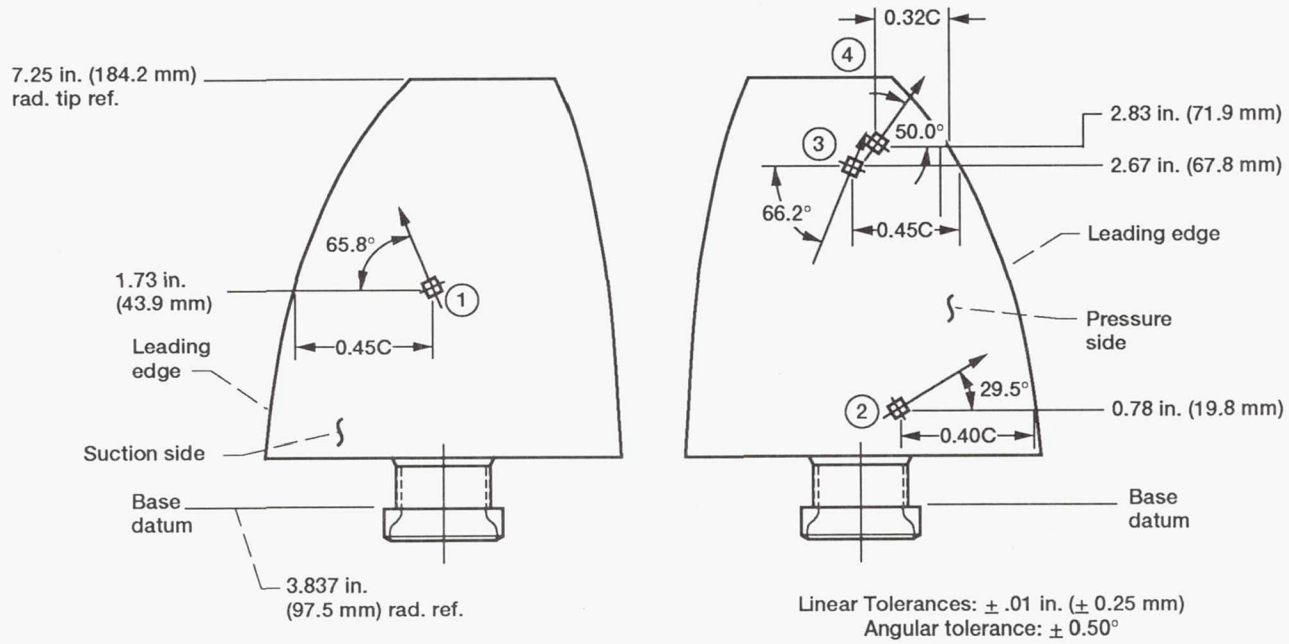

Figure 6.—CM-2D aft blade instrumentation. Arrows indicate orientation of strain gauge. Dimension from leading edge to gauge location is in fraction of chord (C). Dimension from base datum to gauge location is radial (R).

designed to simulate the attachment of the blade in the hub of the propulsion system drive unit. An instrumented CM-1D forward blade and the fixture are shown in figure 7. A cross section of the fixture assembly is shown in figure 8.

The fixture assembly consists of several components. The blade base seats into a circular "saddle" in the fixture base. The saddle is split diametrically to allow for the installation and exchange of blade test specimens. The two halves of the saddle are aligned with dowel pins and are drawn together and held with threaded fasteners. The preload bolt shown in figure 8 is used to apply a force to the blade base. This force presses the blade base into the saddle. By applying different tightening torques, the blade attachment boundary conditions due to differing centrifugal loading are simulated. A washer between the end of the preload bolt and the bottom of the blade base is used to distribute the preload over the blade base evenly. Holes in both the washer and the preload bolt allow for the routing of the strain-gauge lead wires.

The test blade is oriented in the fixture such that the direction of excitation is generally normal to the plane of the airfoil chord. Because these blades have very little airfoil twist, their positioning in the fixture with respect to the direction of excitation was not critical.

Test Equipment

A different combination of test equipment was used for each segment of dynamic testing. Block diagrams of the test equipment configurations for the sine sweep and dwell segments of testing are shown in figures 9 and 10. These figures identify the components used in the tests and the functional relationships between them. The arrows indicate the flow of signals and data between the components.

For the sine sweep resonance survey segment of testing, a sweep oscillator was used to generate a constant-amplitude sinusoidal excitation signal. This signal starts at a frequency below the first predicted mode and sweeps to the ending frequency at a constant rate of 2 octaves per

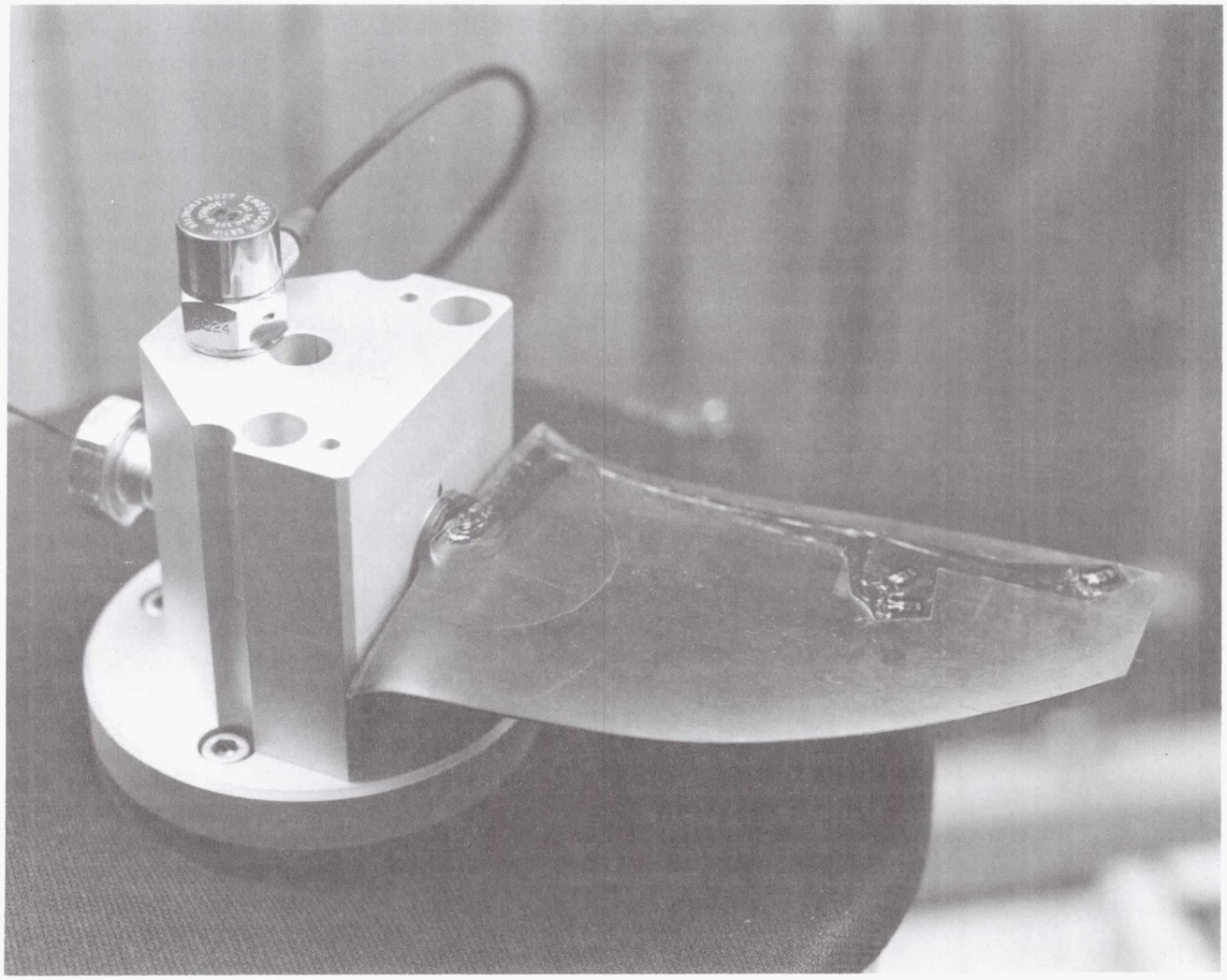

Figure 7.—Instrumented CM-1D forward blade in fixture.

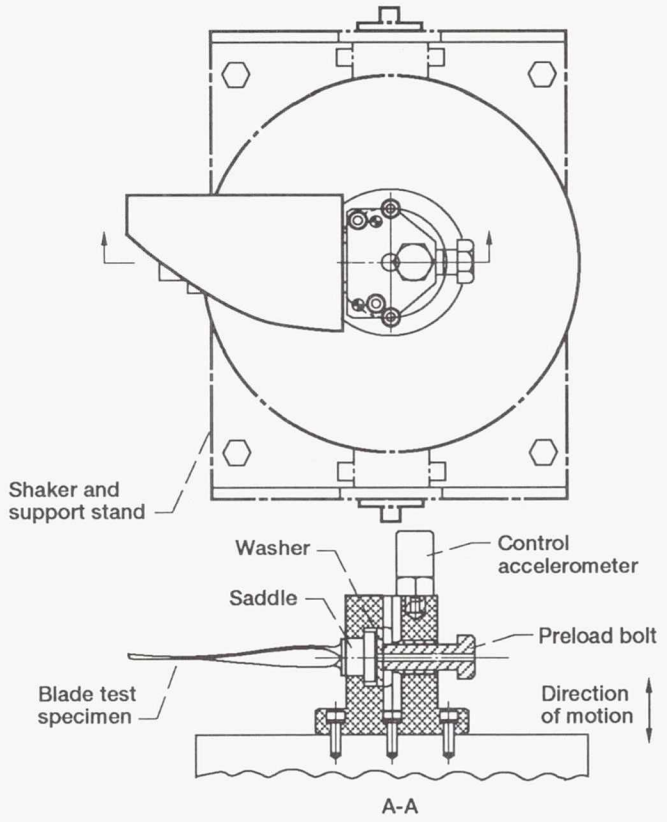

Figure 8.—Fixturing details.

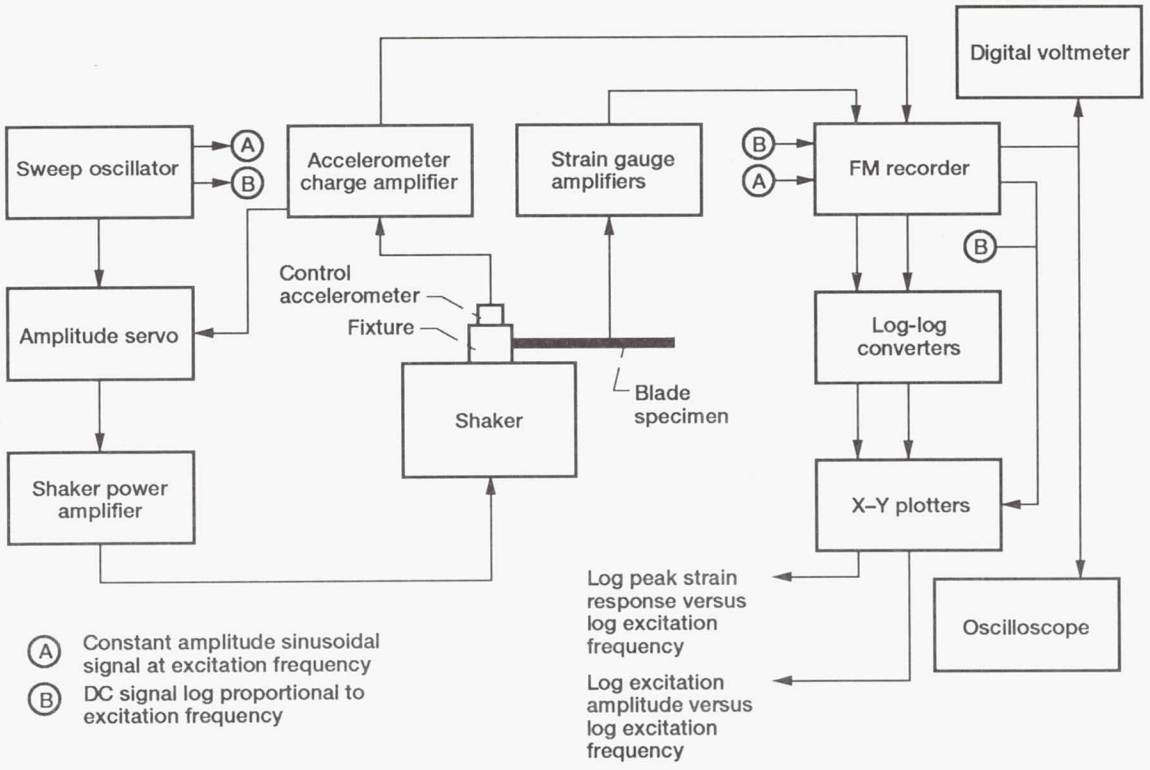

Figure 9.—Sine sweep resonance survey test equipment block diagram.

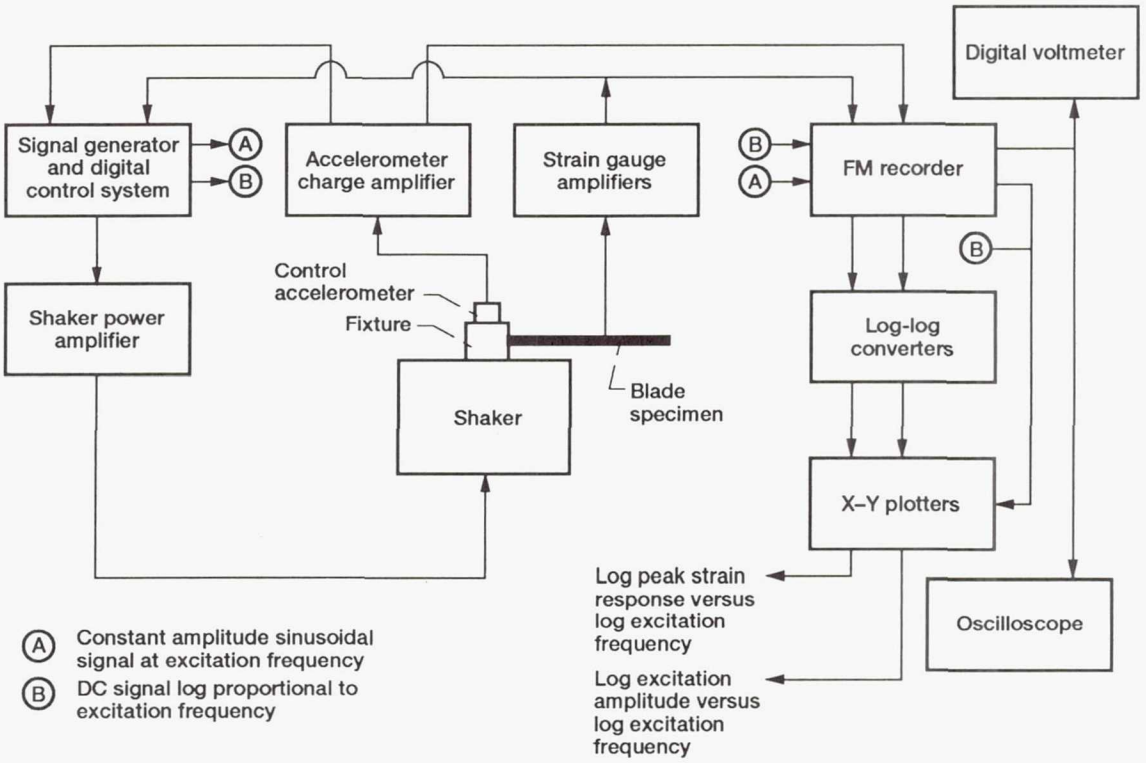

Figure 10.—Dwell test equipment block diagram.

minute. The constant-amplitude excitation signal was routed to an amplitude servo. The amplitude servo was the active control device that adjusted the excitation signal to the desired amplitude. The amplitude servo received a feedback measurement in the form of a signal from the control accelerometer mounted on the test fixture. The sinusoidal excitation signal generated by the sweep oscillator and the amplitude servo was routed to the shaker power amplifier and, in turn, to the shaker.

The strain-gauge response signals and the control accelerometer signal were recorded on FM tape. Both the strain-gauge signals and the control accelerometer signal were played back through log-log converters where the signals were converted to log scale proportional signals. The signals were then routed to *X*-*Y* plotters for plotting of both excitation amplitude and peak strain response versus excitation frequency.

For dwell testing, a combination signal generator and digital controller was used to perform an autophase dwell test. This type of dwell test allows the user to track a specific mode and response amplitude for a specified number of cycles. In the autophase dwell test, the user specifies a frequency close to (in the frequency domain) the resonant frequency of interest. For these tests, the first mode was chosen. When the dwell test sequence begins, the control system automatically performs two sine sweeps close to the user-specified frequency. The system measures and stores the relative response amplitude of the test specimen (in these tests, the strain response at gauge location 1) during these two sweeps. The system then measures both the frequency corresponding to the maximum response amplitude (the resonant frequency) and the relative phase difference between the response and the excitation signals.

Once the frequency and phase corresponding to the resonant condition have been measured, the system begins the dwell test by tracking the phase difference that corresponds to the mode of interest while maintaining the desired response amplitude. The system will, by tracking the phase difference between the response and excitation signals, automatically adjust the excitation frequency if the resonant frequency changes (e.g., due to structural fatigue). The duration of the dwell test is specified by the user in either dwell total elapsed time or the number of cumulative response cycles. Test elapsed time was specified for these blade dwell tests. Both the control accelerometer and strain-gauge signals were recorded once every 5 min on FM tape. The tape serves as a record of both blade peak strain response at the various gauge locations and resonant frequency versus elapsed test time.

Test Matrix

The various tests performed on each blade design are defined in the test matrix presented in table I. The sine sweep resonance survey segment was a series of tests performed at two peak acceleration excitation levels and two base preloads. The tests were designed (1) to deter-

TABLE I.—LRCSW BLADE DYNAMIC TEST MATRIX

Test performed	CM-1D		CM-2D	
	Forward	Aft	Forward	Aft
Resonance survey tests:				
1*g* Sine sweep; 300–4000 Hz; 2 oct./min; base preload, 1000 lb	X	X	X	X
10*g* Sine sweep; 300–4000 Hz; 2 oct./min; base preload, 1000 lb	X	X	X	X
1*g* Sine sweep; 300–4000 Hz; 2 oct./min; base preload, 500 lb		X		
10*g* Sine sweep; 300–4000 Hz; 2 oct./min; base preload, 500 lb		X		
Dwell tests:				
Predwell; 1*g* Sine sweep; 300–3000 Hz; 2 oct./min; base preload, 1000 lb	X		X	
Dwell; 10 million cycles 1200 micro in./in. base preload, 1000 lb	X		X	
Postdwell; 1*g* Sine sweep; 300–3000 Hz; 2 oct./min; base preload, 1000 lb	X		X	

mine the blades' resonant frequencies and modal strain ratios for the first four modes in the range 300 to 4000 Hz; (2) to assess changes, if any, in the blades' resonant frequencies and modal ratios for different excitation amplitudes; (3) to assess the changes, if any, to the blade resonant frequencies and modal ratios due to changes in the applied base preload.

Dwell testing was conducted to demonstrate the endurance capability of each blade design. Because the forward and aft designs for the CM-1D and CM-2D blades have similar geometry and dynamic characteristics, only the forward blade of each design was tested. This segment consisted of three interrelated parts: First, a 1*g* sine sweep was performed before the dwell test to establish the predwell blade resonant frequencies and modal strain ratios. Second, the blades were dwell tested for 10 million cycles at their respective first modes and at an excitation amplitude sufficient to maintain 1200 microstrain at gauge location 1. Strain gauge 1 (SG1) corresponds to the location of maximum predicted principal strain for the first mode of each blade. Finally, after each dwell test, another 1*g* sine sweep test was performed to establish the postdwell condition resonant frequencies and modal ratios. Both the pre- and postdwell sine sweep tests were conducted from 300 to 3000 Hz. The upper frequency bound for these tests was restricted to 3000 Hz by the limitations of the larger shaker used for the dwell phase of testing.

Results and Discussion

Sine Sweep Resonance Survey

A large quantity of strain versus frequency data was acquired during the resonance survey segment of the test program. The peak strain response for the 1*g* excitation amplitude sine sweep test of the CM-1D forward blade is shown in figure 11 as an example of the acquired data. The response plot has several characteristics: First, because of the analog nature of the FM data acquisition system, an inherent base noise level was associated with the strain-gauge response signal. In this example plot, the noise level corresponded to approximately 1.7 microstrain. The blade resonances, or modes, are characterized by a significant deviation of the signal from the base noise level. As the excitation frequency nears a blade resonant frequency, the blade response amplitude increases. This amplitude increase is observed as an increase in the strain response of the blade. The blade resonant frequencies are identified as the frequencies at which there is a maximum in the peak strain response.

The blade resonant frequencies, resonant peak strain responses, and calculated modal ratios for the four blade designs are presented in tables II to V. These tables summarize the results of both the 1*g* and 10*g* excitation sine sweep resonance survey tests in the frequency domain of 300 to 4000 Hz with the nominal base preload of 1000 lb. Only significant blade modes are identified.

Because the positions of the strain gauges were chosen based on analytical predictions of maximum principal strain for each of the first four modes, only one strain gauge is at the location, and in the direction, of the maximum strain for each of the first four modes. The remaining three gauges, for a given mode, are off-axis and consequently measure lower response amplitudes. In several tests the off-axis gauges produced response signals comparable to the base noise level; thus, this off-axis data must be viewed with caution because the response signal may contain significant noise contribution.

There are instances where modal ratios for a particular gauge location and mode could not be calculated either because of the lack of significant response or because of bad data (identified as footnotes to tables II to V). Note that, for the CM-2D forward and aft blade 1*g* sine sweep tests, little meaningful data were taken (tables IV and V). The shorter length and greater stiffness of the CM-2D blades produced strain responses below the FM recorder noise floor. In retrospect, it would have been useful to perform another series of 1*g* sine sweep tests with different recording calibration levels to "pull" the response signals out of the FM recorder noise floor.

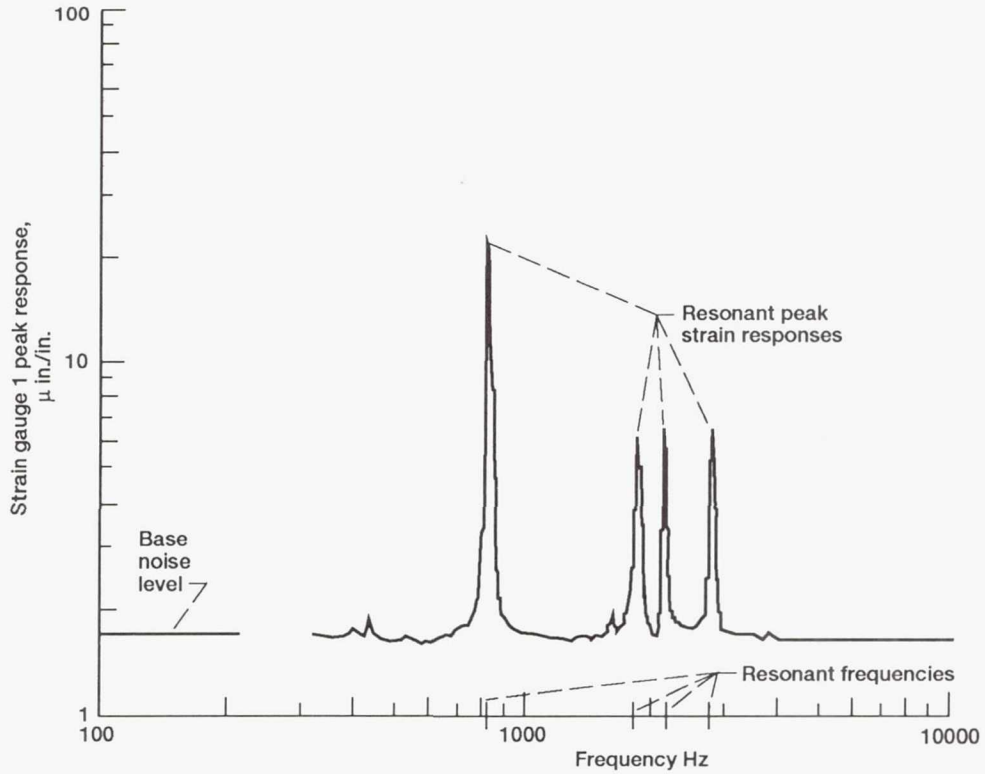

Figure 11.—CM-1D forward sine sweep response. Sine sweep, 1g; frequency range, 300–4000 Hz; sweep rate, 2 octaves per minute; base preload, 1000 lb..

TABLE II.—CM-1D FORWARD BLADE RESONANCE SURVEY TEST RESULTS

[Base preload, 1000 lb.]

Gauge location	1*g* Sine sweep				10*g* Sine sweep			
	Mode							
	1	2	3	4	1	2	3	4
	Resonant frequency, Hz							
	820	1850	2100	2750	820	1850	2150	2800
	Peak strain response, μin./in.							
1	45.0	8.0	9.0	[a]3.2	340.0	98.0	86.0	28.0
2	22.5	6.4	6.6	6.6	150.0	78.0	64.0	66.0
3	30.0	9.8	[a]3.5	11.0	190.0	115.0	[a]25.0	110.0
4	19.0	7.8	[a]3.5	11.0	130.0	96.0	38.0	110.0
	Modal ratios[b]							
1	1.00	1.00	1.00	[a]1.00	1.00	1.00	1.00	1.00
2	.50	.80	.73	[a]2.06	.44	.80	.76	2.36
3	.67	1.23	[a].39	[a]3.44	.56	1.17	[a].29	3.93
4	.42	.98	[a].39	[a]3.44	.38	.98	.44	3.93

[a]Recorded signal below 3 × base noise level. Value may contain significant noise contribution.
[b]Resonant peak strain normalized with respect to location 1.

TABLE III.—CM-1D AFT BLADE RESONANCE SURVEY TEST RESULTS

[Base preload, 1000 lb.]

Gauge location	1g Sine sweep				10g Sine sweep			
	Mode							
	1	2	3	4	1	2	3	4
	Resonant frequency, Hz							
	780	1600	2100	2500	780	1600	2050	2500
	Peak strain response, μin./in.							
1	------Bad data------				880.0	130.0	100.0	67.0
2	13.0	[a]3.5	(b)	[a]4.4	630.0	165.0	60.0	124.0
3	[a]4.5	(b)	(b)	[a]4.1	185.0	76.0	70.0	205.0
4	8.0	(b)	(b)	[a]3.6	390.0	105.0	71.0	155.0
	Modal ratios[c]							
1	(d)	(d)	(d)	(d)	1.00	1.00	1.00	1.00
2	↓	↓	↓	↓	.72	1.27	.60	1.85
3	↓	↓	↓	↓	.21	.59	.70	3.06
4	↓	↓	↓	↓	.44	.81	.71	2.31

[a]Recorded peak strain response signal below 3 × base noise level. Value may contain significant noise contribution.

[b]No significant response observed.

[c]Resonant peak strain normalized with respect to gauge location 1.

[d]No modal ratio calculated.

TABLE IV.—CM-2D FORWARD BLADE RESONANCE SURVEY TEST RESULTS

[Base preload, 1000 lb.]

Gauge location	1g Sine sweep					10g Sine sweep				
	Mode									
	1	2	3	4	5	1	2	3	4	5
	Resonant frequency, Hz									
	940	-----	-----	-----	-----	920	1600	1700	2400	3300
	Peak strain response, μin./in.									
1	46.0	(a)	(a)	(a)	(a)	390.0	[b]12.0	[b]12.0	17.5	[b]7.7
2	33.0	↓	↓	↓	↓	245.0	[b]11.5	[b]14.5	37.0	[b]9.0
3	24.0	↓	↓	↓	↓	185.0	[b]9.7	[b]9.6	47.0	[b]9.9
4	11.0	↓	↓	↓	↓	70.0	[b]9.4	[b]11.0	23.0	17.5
	Modal ratios[c]									
1	1.00	(a)	(a)	(a)	(a)	1.00	[b]1.00	[b]1.00	1.00	[b]1.00
2	.72	↓	↓	↓	↓	.63	[b].96	[b]1.21	2.11	[b]1.17
3	.52	↓	↓	↓	↓	.47	[b].81	[b].80	2.69	[b]1.29
4	.24	↓	↓	↓	↓	.18	[b].78	[b].92	1.31	[b]2.27

[a]No significant response observed.

[b]Recorded signal below 3 × base noise level. Value may contain significant noise contribution.

[c]Resonant peak strain normalized with respect to gauge location 1.

TABLE V.—CM-2D AFT BLADE RESONANCE SURVEY TEST RESULTS

[Base preload, 1000 lb.]

Gauge location	1g Sine sweep				10g Sine sweep			
	Mode							
	1	2	3	4	1	2	3	4
	Resonant frequency, Hz							
	930	1800	2350	3000	930	1800	2350	3000
	Peak strain response, μin./in.							
1	54.0	(a)	2.9	(a)	440.0	(a)	30.0	[b]8.0
2	58.0	[b]1.6	14.0	2.2	450.0	12.5	130.0	19.0
3	21.0	(a)	6.3	5.5	215.0	[b]10.0	74.0	65.0
4	16.0	[b]1.0	5.0	7.8	135.0	[b]9.4	48.0	76.0
	Modal ratios[c]							
1	1.00	(d)	1.00	(d)	1.00	(d)	1.00	[b]1.00
2	1.07	↓	4.83	↓	1.02	↓	4.33	[b]2.38
3	.39	↓	2.17	↓	.49	↓	2.47	[b]8.13
4	.30	↓	1.72	↓	.31	↓	1.60	[b]9.50

[a]No significant response observed.

[b]Recorded peak strain response signal below 3 × base noise level. Value may contain significant noise contribution.

[c]Resonant peak strain normalized with respect to gauge location 1.

[d]No modal ratio calculated.

TABLE VI.—COMPARISON OF STRAIN RESPONSES TAKEN AT PEAK EXCITATIONS OF 1g AND 10g

[Base preload, 1000 lb.]

Gauge location	CM-1D forward				CM-2D aft			
	Mode							
	1	2	3	4	1	2	3	4
	Resonant frequency, Hz							
	820	1850	2100	2750	930	1800	2350	3000
	Peak strain response (PSR) ratio, PSR_{10g}/PSR_{1g}							
1	7.56	12.25	9.56	[a]8.75	8.15	(b)	10.35	(b)
2	6.67	12.18	9.70	10.00	7.76	[a]7.81	9.29	8.64
3	6.33	11.74	[a]7.14	10.00	10.24	(b)	11.75	11.82
4	6.84	12.31	10.86	10.00	8.44	[a]9.40	9.60	9.74
Average	6.85	12.12	8.80	10.00	8.65	(b)	10.25	10.07

[a]Recorded signal below 3 × base noise level. Value may contain significant noise contribution. Ignored in calculation of averages.

[b]No ratio calculated due to lack of significant response.

A comparison of the 1*g* and 10*g* sine sweep response data for the CM-1D forward and CM-2D aft blades was made to assess the effects of different excitation *g* levels. Table VI summarizes the ratio of the resonant peak strain response for a given gauge location and mode for the 10*g* test to the resonant peak strain response for the same gauge location and mode for the 1*g* test for the CM-1D forward and CM-2D aft blades. As expected, the resonant peak strain amplitudes were higher for the 10*g* excitation than for the 1*g* excitation. Of significance is that blade resonances occur at the same frequencies for the two tests. This indicates that the stiffness response, with respect to excitation amplitude, is linear. It was not possible to make a meaningful comparison for the CM-1D aft and CM-2D forward blades because of the lack of significant response and bad recorded data for the 1*g* test for these blades.

The peak strain response ratio is relatively consistent for all four gauges for each mode of the CM-1D forward blade (table VI). The increase in peak strain response between the 1*g* and 10*g* excitation, however, was not comparable from mode to mode. The average strain ratio for a given mode ranged from a low of 6.85 for mode 1 to a high of 12.12 for mode 2. The variability of recorded data from the 1*g* test of the CM-2D aft blade does not allow for similar comparisons.

Sensitivity of the blade response to different base preloads was also evaluated. Both 1*g* and 10*g* sine sweep tests were performed on the CM-1D aft blade with base preloads of 500 and 1000 lbs and the results compared. As with many of the other 1*g* tests, response recorded for the CM-1D aft blade was not significant enough for a meaningful comparison. The 10*g* results were, however, suitable for comparison.

The resonant frequencies, modal strain ratio comparison, and resonant peak strain response amplitude ratios for the CM-1D aft blade at the 500- and 1000-lb base preloads are summarized in table VII. The resonant frequencies for the two base preloads were the same, and the modal strain ratios for a gauge at a mode were comparable. The resonant peak strain responses, on the other hand, were considerably different. In general, the resonant peak strain response for the 500-lb preload test was roughly half the response for the 1000-lb preload test for the 10*g* excitation amplitude. This effect is most likely due to the change in damping at the blade base to fixture interface. The lower base preload allows for more relative movement and, consequently, more Coulomb damping between the blade base and the fixture. A similar trend would be expected for the other blades.

TABLE VII.—CM-1D AFT BLADE SINE SWEEP 10*g* RESONANCE SURVEY, 500-lb PRELOAD VERSUS 1000-lb PRELOAD COMPARISON

Base preload, lb	Gauge location	Mode			
		1	2	3	4
		Resonant frequency, Hz			
		780	1600	2050	2500
		Modal ratio[a]			
500	1	1.00	1.00	1.00	1.00
	2	.82	1.42	.57	3.69
	3	.24	.67	.83	3.02
	4	.47	.83	.69	2.22
1000	1	1.00	1.00	1.00	1.00
	2	.72	1.04	.60	3.58
	3	.21	.59	.70	3.06
	4	.44	.81	.71	2.31

Gauge location	Mode			
	1	2	3	4
	Resonant frequency, Hz			
	780	1600	2050	2500
	Peak strain response (PSR) ration, $PSR_{500\ lb}/PSR_{1000\ lb}$			
1	0.375	0.462	0.420	0.485
2	.429	.515	.400	.500
3	.422	.526	.500	.478
4	.397	.476	.409	.465

[a]Peak strain response at each gauge loction normalized with respect to response at gauge location 1.

Dwell Test

The data acquired during the dwell test segment have been reduced to reveal the changes in blade dynamic response as a result of the high-cycle, high-strain sinusoidal excitation resonance dwell test. Comparisons are made based on pre- and postdwell sine sweep data. Also, trends are identified in the dwell response data.

The CM-1D and CM-2D forward blades' pre- and postdwell sine sweep test results are presented in tables VIII and IX. Comparison of the CM-1D forward pre- and postdwell resonant frequencies indicates a decrease in resonant frequency of approximately 6 percent for the first two modes and decreases of 5 percent and 3 percent for modes 3 and 4, respectively. Comparison of the CM-2D forward pre- and postdwell condition resonant frequencies indicates a decrease in resonant frequency of approximately 1.5 percent for each of the first three modes.

Table X presents the pre- and postdwell condition modal ratios for the CM-1D and CM-2D forward blades. There was no significant change in the modal strain ratios of the CM-1D forward blade. For gauge locations 3 and 4

TABLE VIII.—CM-1D FORWARD BLADE PRE- AND POSTDWELL DYNAMIC CHARACTERISTICS COMPARISONS

[1*g* Sine sweep; base preload, 1000 lb.]

Mode	Resonant frequency, Hz		Resonant peak strain response, μin./in., at strain gauge (SG) location							
			SG1		SG2		SG3		SG4	
	Pre-dwell	Post-dwell	Pre-dwell	Post-dwell	Pre-dwell	Post-dwell	Pre-dwell	Post-dwell	Pre-dwell	Post-dwell
1	812	762	63.0	[a]41.0	31.5	21.0	39.0	[a]28.0	24.0	15.5
2	1776	1663	21.0	[a]16.0	17.5	12.0	22.5	[a]15.5	18.0	11.5
3	2081	1976	8.6	[a]5.4	7.0	4.4	3.8	[a]1.7	3.2	2.3
4	2700	2620	1.9	[a]1.9	4.1	3.8	5.2	[a]5.0	5.4	5.0

Mode	$\frac{\text{Postwell value - predwell value}}{\text{predwell value}} \times 100 = \text{percent}$				
	F	SG1	SG2	SG3	SG4
1	−6.2	−34.9	−33.3	−28.2	−35.4
2	−6.4	−23.8	−31.4	−31.1	−36.1
3	−5.0	−37.2	−37.1	−55.3	−28.1
4	−3.0	0.0	−7.3	−3.9	−7.4

[a]Values showed significant degradation during dwell test.

TABLE IX.—CM-2D FORWARD BLADE PRE- AND POSTDWELL DYNAMIC CHARACTERISTICS COMPARISONS

[1*g* Sine sweep; base preload, 1000 lb.]

Mode	Resonant frequency, Hz		Resonant peak strain response, μin./in., at strain gauge (SG) location							
			SG1		SG2		SG3		SG4	
	Pre-dwell	Post-dwell	Pre-dwell	Post-dwell	Pre-dwell	Post-dwell	Pre-dwell	Post-dwell	Pre-dwell	Post-dwell
1	935	921	69.0	[a]59.0	43.0	(b)	35.0	30.0	12.5	11.0
2	1673	1648	4.0	[a]4.8	5.7	(b)	2.5	3.0	4.0	4.9
3	2359	2322	3.2	[a]3.2	6.9	(b)	8.0	8.0	4.2	4.6

Mode	$\frac{\text{Postwell value - predwell value}}{\text{predwell value}} \times 100 = \text{percent}$				
	F	SG1	SG2	SG3	SG4
1	−1.5	−14.5	(b)	−14.3	−12.0
2	−1.5	+20.0	(b)	+20.0	+22.5
3	−1.6	0.0	(b)	0.0	+9.5

[a]Peak strain values from gauge that showed significant signal degradation during high-level dwell test.

[b]No intelligible data taken.

TABLE X.—CM-1D AND CM-2D FORWARD BLADE PRE- AND POSTDWELL MODAL RATIO COMPARISONS

[1g Sine sweep; base preload, 1000 lb.]

(a) CM-1D forward blade

Mode	Resonant frequency, Hz		Modal ratios,[a] at strain gauge location							
			SG1		SG2		SG3		SG4	
	Pre-dwell	Post-dwell	Pre-dwell	Post-dwell	Pre-dwell	Post-dwell	Pre-dwell	Post-dwell	Pre-dwell	Post-dwell
1	812	762	1.00	[b]1.00	0.50	0.51	0.62	[b]0.68	0.38	0.38
2	1776	1663	↓	↓	.83	.75	1.07	[b].97	.86	.72
3	2081	1976	↓	↓	.81	.82	.44	[b].32	.37	.43
4	2700	2620	↓	↓	2.16	2.00	2.74	[b]2.63	2.84	2.63

(b) CM-2D forward blade

1	935	921	1.00	[b]1.00	0.62	(c)	0.51	0.51	0.18	0.19
2	1673	1648	1.00	[b]1.00	1.43	(c)	.63	.63	1.00	1.02
3	2359	2322	1.00	[b]1.00	2.16	(c)	2.50	2.50	1.31	1.44

[a]Resonant peak strain response normalized with respect to gauge location 1.
[b]Peak strain values from gauge that showed significant signal degradation during dwell test.
[c]No intelligible data taken.

on the CM-2D blade there was also no significant change in modal strain response from the pre- to postdwell condition. Because of the deterioration of the strain gauge at location 2 on the CM-2D forward blade during the dwell test, no intelligible data were taken in the postdwell sine sweep test.

For both the CM-1D and CM-2D forward blades, the resonant peak strain responses for the postdwell 1g sine sweep tests were lower than the corresponding resonant peak strain responses for the predwell 1g sine sweep tests. This trend indicates an increase in the system damping from the pre- to the postdwell condition for both blades. Both the decrease in resonant frequencies and the increase in damping indicate that structural deterioration was occurring in both blades due to accumulated fatigue damage.

Degradation of the strain gauge signal used for control of the dwell test for both forward blades necessitated interrupting each test to reconfigure to another gauge location for control. Initially, all strain gauges produced clean, symmetrical, sinusoidal response signals during the dwell test. As the test continued, the signal from the control strain gauge (gauge location 1, which experienced the maximum strain) began to degrade. This degradation was first evidenced by an unsymmetrical response waveform, which indicates that the compression response of the strain gauge was different from the tension response. Previous high-strain test experience has shown that solder joint cracking may cause such a trend. It might also have been caused by a progressive debonding of the control strain gauge from the surface of the blade. Posttest visual inspection indicated no obvious anomalies.

As the tests progressed, the strain-control signal waveforms became increasingly jagged and irregular. A study of the literature concerning the characteristics of the control system (ref. 6) indicates that, for structures having a high resonant amplification factor, the system has difficulty tracking the phase difference between the excitation and response signals when the response signal becomes "dirty." As the strain signal degraded further, the control system began to experience difficulty in tracking the resonant condition phase difference and response amplitude. When this condition occurred, the test was interrupted to reconfigure to a strain gauge that exhibited a clean response signal.

When the test was interrupted, a new control channel, a new gauge location, and new peak strain set point were chosen for control. The new control gauge was selected by first reviewing the most recently acquired response signal waveforms of gauges 2, 3, and 4 and then selecting one that was producing a clean, symmetrical, sinusoidal signal. For the CM-1D blade, gauge 2 was chosen, while for the CM-2D blade, gauge 3 was used. The peak strain response set point for control was chosen based on the response of the chosen gauge location just before test interruption in the belief, not only that peak strain amplitude would vary, but also that the modal strain distribution would be changing as a result of cumulative fatigue damage. The dwell test was then restarted with control from the new control gauge location and peak strain set point.

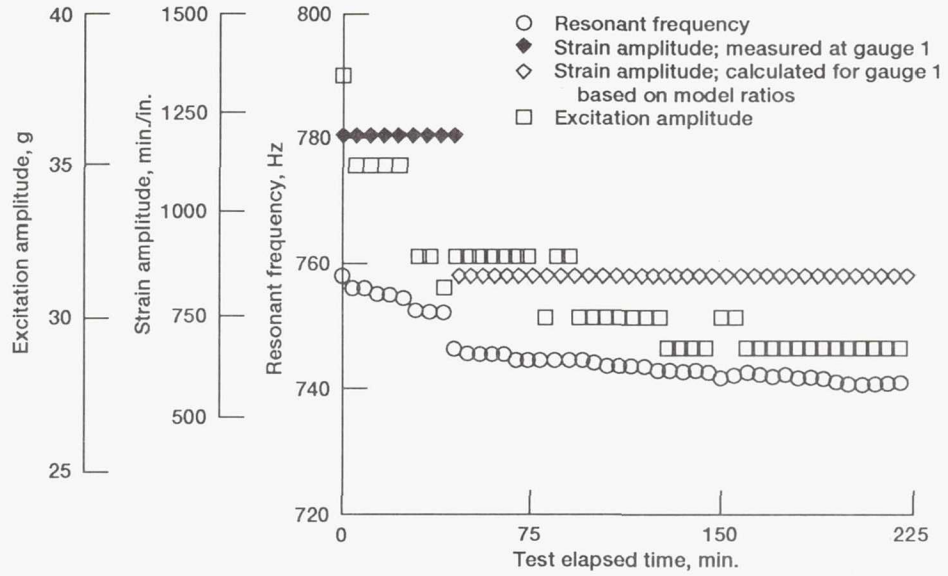

Figure 12.—CM-1D forward resonant frequency, strain amplitude, and excitation amplitude versus dwell test elapsed time.

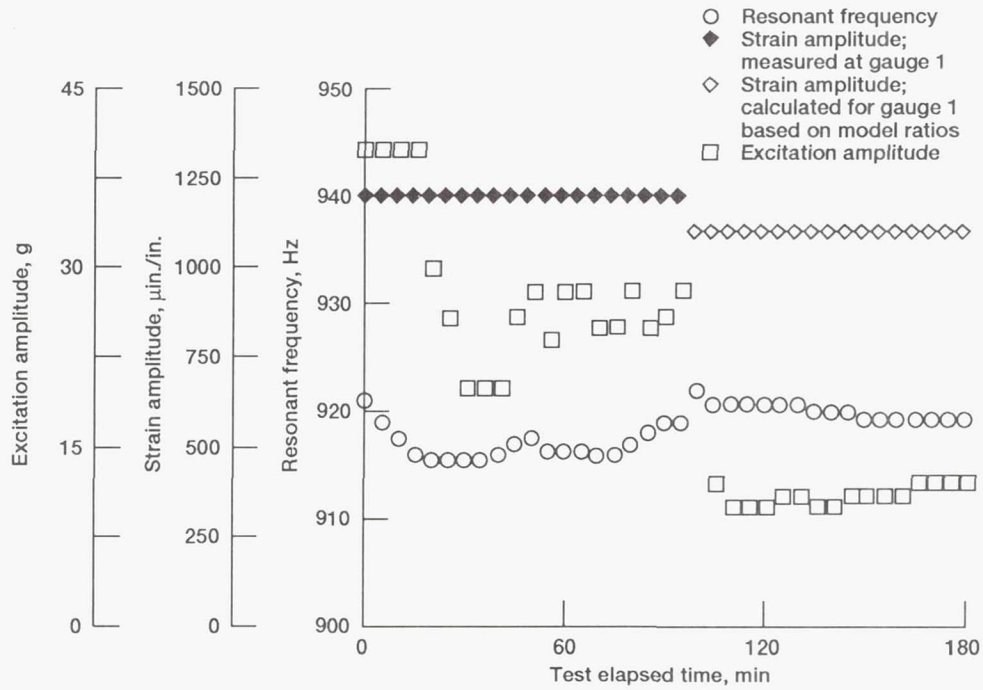

Figure 13.—CM-2D forward resonant frequency, strain amplitude, and excitation amplitude versus dwell test elapsed time.

The blade resonant frequency, maximum resonant peak strain response amplitude, and excitation amplitude as functions of the dwell test elapsed time for the CM-1D and CM-2D forward blades are presented in figures 12 and 13. A review of the peak strain response data indicates that after the tests were reconfigured to control from a new strain-gauge location, the maximum strain level achieved was below the desired maximum of 1200 microstrain.

As mentioned previously, the peak strain response set point for control was chosen based on the response of the new control gauge location just before dwell test interruption. The control system at that time, with both frequency and amplitude tracking deteriorating, was having difficulty maintaining the resonant condition. Thus, the peak strain responses at the four strain-gauge locations were lower than the values that would correspond to the desired maximum peak strain response of 1200 microstrain. It is these lower values on which the new maximum strain control set point was based.

A review of the modal ratios calculated based on pre-

TABLE XI.—CM-1D AND CM-2D FORWARD DWELL TEST MAXIMUM PEAK STRAIN RESPONSE AND CUMULATIVE CYCLES

Forward blade	Peak strain response, μin./in.	Cumulative cycles	Test duration, percent
CM-1D	[a]1200	5.52×10^6	55.2
	[b]860	4.48×10^6	44.8
CM-2D	[a]1200	2.73×10^6	27.3
	[b]1120	7.27×10^6	72.7

[a]Measured at gauge 1 before gauge failure.
[b]Calculated at gauge 1 based on modal ratios after gauge failure.

dwell sine sweep, initial dwell, and postdwell sine sweep resonant peak strain values (see table XI) indicates very little change in the blade strain response ratio from the pre- to postdwell condition. Although the blades were undertested with respect to the peak strain level maintained during the dwell test, the data collected were sufficient to allow us to set maximum strain limits for the wind tunnel tests.

The control problems encountered during the dwell testing were a result of the limited useful life of the strain gauge (and/or the attachment of the strain gauge to the test specimen) for a high-level high-cycle test. Because the modal strain distribution did not change, it would have been more appropriate to review the resonant peak strain data at each gauge location at the beginning of the dwell test. At that time the control system was tracking the resonant condition, and the resonant peak strain response at each strain-gauge location was consistent with the desired maximum peak strain response of 1200 microstrain at strain gauge location 1. A set point based on these data would have resulted in maintaining the desired maximum strain amplitude throughout the dwell test.

Another option for avoiding control problems is to use a gauge location other than the one experiencing maximum strain for control. To select an appropriate control gauge, a low-cycle, dwell test, controlled from the gauge location experiencing the desired maximum strain, would be performed to establish the resonant peak strain response at each gauge location. The peak strain response at the other gauge locations would then correspond to the desired maximum strain response associated with that mode. The test could then be reconfigured to control from one of these other gauge locations with a set point consistent with the desired maximum peak strain. The control gauge experiencing a peak strain level lower than the maximum should, all other factors being equal, not deteriorate as quickly as the gauge at the location of maximum peak strain.

Summary of Results

A dynamic test program was conceived and executed in support of the development of a cruise missile propulsion concept for the Navy. This program investigated the characteristics of four scale-model composite propfan blade designs. The areas investigated included blade resonant frequencies, modal strain distributions, and strain endurance capabilities.

The first goal of the test program was to characterize the as-built dynamics of the blades. A series of sine sweep resonance survey tests were performed. The results of these tests established the as-built resonant frequencies and modal strain ratios in the frequency range of 300 to 4000 Hz for each blade tested. The tests were also used to assess the effect of excitation level and blade base preload on the blades' dynamic characteristics.

Comparison of $1g$ and $10g$ peak excitation level sine sweep test results was made to assess the effects of different excitation levels on the blades' dynamic characteristics. The results indicated that the stiffness response of the blades is linear (same frequencies). In addition, comparison of the modal ratios calculated for each test showed that the modal strain distributions for the two excitation levels were comparable for a particular mode. The mode to mode amplitude response varied.

Sine sweep tests at the same excitation level but for two different base preloads were performed on the CM-1D aft blade to assess the effects of different base preloads on the blades' dynamic characteristics. The resonant frequencies for the two base preloads were the same. For the same excitation level, the test conducted with the lower base preload resulted in lower response amplitudes. This is most likely due to an increase in damping at the blade to fixture interface associated with the lower base preload. Because the four blade designs are of similar geometry and construction, a similar trend would be expected for the other blade designs.

The second goal of the test program was to demonstrate an acceptable maximum strain operating limit for each blade design for use during subsequent wind tunnel tests. A high-level (1200 microstrain), high-cycle (10 million cycles), dwell test was performed on the CM-1D and CM-2D forward blades. Pre- and postdwell sine sweep tests were performed on each blade to establish pre- and postdwell dynamic characteristics.

Difficulties in controlling the dwell test resulted in both the CM-1D and CM-2D forward blades being undertested with respect to the maximum strain level selected. Results were, however, sufficient for setting wind tunnel test strain limits.

The pre- and postdwell sine sweep test results showed that, for both the CM-1D and CM-2D forward blades,

resonant frequencies and peak strain responses decreased due to the high-strain dwell input. In all cases, the decrease in frequency was less than the chosen failure criteria. The modal strain ratios were comparable from the pre- to postdwell condition, which indicates that the accumulated structural fatigue did not significantly affect the blades' modal response. The change in resonant peak strain response signified an increase in system damping from the pre- to postdwell condition. The decrease in resonant frequencies and the increase in damping also indicated that some structural deterioration was incurred as a result of the dwell test.

References

1. Krzycki, L.J.; and Strutz, L.W.: Analytical and Experimental Investigation of Propfan Propulsion for Cruise Missiles. NWC–TM–6948, Naval Weapons Center, 1991.
2. Ernst, M.: Structural Analysis of Low RPM Composition Propfan Blades for the LRCSW Wind Tunnel Model. NASA TM–105266, 1992.
3. Carek, D.A.: Structural Analysis of High RPM Composite Propfan Blades for a Cruise Missile Wind Tunnel Model. NASA TM–105267, 1991.
4. Strain Gage Selection Criteria, Procedures, Recommendations. TN–505. Measurements Group Inc., Raleigh, NC, 1983.
5. Fatigue Characteristics of Micro-Measurements Strain Gages. TN–508. Measurements Group Inc., Raleigh, NC, 1982.
6. Anathanarayanan, K.: Technical Considerations in Automatic Resonance Dwell Testing. Proceedings, 33rd Annual Technical Meeting, Institute of Environmental Sciences, 1987, pp. 256-262.

REPORT DOCUMENTATION PAGE

Form Approved
OMB No. 0704-0188

Public reporting burden for this collection of information is estimated to average 1 hour per response, including the time for reviewing instructions, searching existing data sources, gathering and maintaining the data needed, and completing and reviewing the collection of information. Send comments regarding this burden estimate or any other aspect of this collection of information, including suggestions for reducing this burden, to Washington Headquarters Services, Directorate for information Operations and Reports, 1215 Jefferson Davis Highway, Suite 1204, Arlington, VA 22202-4302, and to the Office of Management and Budget, Paperwork Reduction Project (0704-0188), Washington, DC 20503.

1. AGENCY USE ONLY (*Leave blank*)	2. REPORT DATE	3. REPORT TYPE AND DATES COVERED
	February 1993	Technical Memorandum

4. TITLE AND SUBTITLE

Structural Dynamic Testing of Composite Propfan Blades for a Cruise Missile Wind Tunnel Model

5. FUNDING NUMBERS

WU–535–03–0B

6. AUTHOR(S)

Stephen D. Elgin and Thomas J. Sutliff

7. PERFORMING ORGANIZATION NAME(S) AND ADDRESS(ES)

National Aeronautics and Space Administration
Lewis Research Center
Cleveland, Ohio 44135–3191

8. PERFORMING ORGANIZATION REPORT NUMBER

E–6663

9. SPONSORING/MONITORING AGENCY NAMES(S) AND ADDRESS(ES)

National Aeronautics and Space Administration
Washington, D.C. 20546–0001

10. SPONSORING/MONITORING AGENCY REPORT NUMBER

NASA TM–105272

11. SUPPLEMENTARY NOTES

Responsible person, Stephen D. Elgin, (216) 433–3895.

12a. DISTRIBUTION/AVAILABILITY STATEMENT

Unclassified - Unlimited
Subject Categories 05 and 39

12b. DISTRIBUTION CODE

13. ABSTRACT ***(Maximum 200 words)***

The Naval Weapons Center at China Lake, California is currently evaluating a counter rotating propfan system as a means of propulsion for the next generation of cruise missiles. The details and results of a structural dynamic test program are presented for scale model graphite–epoxy composite propfan blades. These blades are intended for use on a cruise missile wind tunnel model. Both dynamic characteristics and strain operating limits of the blades are presented. Complications associated with high strain level fatigue testing methods are also discussed.

14. SUBJECT TERMS

Vibration; Vibration tests; Propfan technology; Composite materials

15. NUMBER OF PAGES

20

16. PRICE CODE

A03

17. SECURITY CLASSIFICATION OF REPORT	18. SECURITY CLASSIFICATION OF THIS PAGE	19. SECURITY CLASSIFICATION OF ABSTRACT	20. LIMITATION OF ABSTRACT
Unclassified	Unclassified	Unclassified	

National Aeronautics and
Space Administration

Lewis Research Center
Cleveland, Ohio 44135

FOURTH CLASS MAIL

ADDRESS CORRECTION REQUESTED

Official Business
Penalty for Private Use $300

Postage and Fees Paid
National Aeronautics and
Space Administration
NASA 451

NASA